PHYSICAL REVIEW B **81**, 140403(R) (2010)

Low spin moment due to hidden multipole order from spin-orbital ordering in LaFeAsO

Francesco Cricchio, Oscar Grånäs, and Lars Nordström
Department of Physics and Astronomy, Uppsala University, P.O. Box 516, 751 20 Uppsala, Sweden
(Received 21 January 2010; revised manuscript received 1 March 2010; published 13 April 2010)

An antiferromagnetic (AF) low-moment solution, $0.35\mu_B$/Fe, is found in the case of LaOFeAs for an intermediately strong Coulomb interaction U of 2.75 eV. This solution is stabilized over a large moment solution due to the gain in exchange energy in the formation of large multipoles of the spin magnetization density. The multipoles are of rank four and can be understood as a type of spin-orbital ordering. Parallels can be drawn to the stabilization of the AF order in, e.g., $CaCuO_2$.

DOI: 10.1103/PhysRevB.81.140403 PACS number(s): 75.25.−j, 74.70.Xa, 75.10.Lp

With the discovery of the iron pnictide layered superconductors in 2008,[1] a hope was quickly raised that these materials would finally lead to an understanding of the elusive mechanism of the superconductivity of the high-T_C cuprates. Indeed there are many common features; the fact that the parent compound is antiferromagnetic (AF), the central role played by a transition-metal layer, the fact that the AF order quickly disappears with doping and then is overtaken by a strong superconducting state. However, fairly soon some differences were also discovered. While the main electrons in the cuprates are correlated and close to an insulating state, in the iron pnictides they seems to be at most moderately correlated and metallic.[2,3] This difference between the two types of materials is also manifested by the fact that density-functional theory (DFT) based calculations of the undoped iron pnictides obtain the correct metallic AF order while in the undoped cuprates they falsely lead to a nonmagnetic metallic state. When a correlation term is added to the DFT Hamiltonian, local-density approximation plus added Coulomb U interaction formalism (LDA+U), an AF insulating phase is obtained.[4] However, with the increasing number of DFT studies, it has been clarified that DFT has problems also for the iron pnictide parent compounds, although of different nature.[5] The calculations systematically predict unusually bad Fe-As bonding distances and overestimate the ordered AF spin moment, which is $0.35\mu_B$ in LaOFeAs.[6] In fact, state-of-the-art DFT calculations in the generalized gradient approximation (GGA) give spin moments of the order $2.0–2.5\mu_B$,[5,7] i.e., an overestimation by at least a factor 5.

In this Rapid Communication we perform LDA+U calculation for the AF parent compound LaOFeAs. The obtained results show that, for realistic U parameters, a low spin moment solution is stabilized due to polarization of higher multipole moments of the spin density. These terms can be analyzed as a spin-orbital ordering among mainly the xz and yz d orbitals at the Fe sites. It is also found that the calculated equilibrium distance between the Fe plane and the As planes is in good agreement with the experimental value.[6] Finally we make a comparison with the LDA+U solution for an undoped cuprate, $CaCuO_2$, which reveals a striking similarity in the role played by magnetic multipoles.

The electronic structure is calculated within the full-potential augmented plane wave plus local orbital method as implemented in the ELK code.[8] The LDA+U approach is applied following the same methodology as described in Ref. 9 with Yukawa screening[10] and around mean-field double counting while the GGA (Ref. 11) is used for the DFT part. The AF Brillouin zone (BZ) is sampled with $10\times10\times6$ $\vec{k}$ points uniformly spaced. The calculations are done for the crystal parameters of the experimental high-temperature tetragonal structure,[6] except when optimizing the internal z_{As} parameter. The parameter governing the number of augmented plane waves $R|\vec{G}+\vec{k}|_{max}$ is set to 8.0, where R is the Fe muffin-tin radius and $\vec{G}$ are the reciprocal-lattice vectors.

There have been several attempts to estimate the magnitude of the Coulomb interaction U in this compound. The results stretch all the way from fairly large values of 4 eV leading to strong correlation,[12] through moderate values of 3–4 eV (Ref. 13) and 2.7 eV,[14] down to less than 2 eV.[15] As has been discussed,[13,14] part of the disagreement stems from the different choices of band manifolds that are allowed to interact with this Coulomb interaction. If one performs a downfolding to a subset of Fe d states the effective Coulomb interaction has to be decreased too, otherwise the correlation effect is overestimated. In the present study we will vary U between 0 and 4 eV, where the $U=0$ eV case corresponds to a pure GGA calculation, since all Slater parameters are screened with the same Yukawa screening length.[9] In this approach the Hund's rule exchange parameter J varies automatically between 0 and 1 eV, with, e.g., $J=0.86$ eV for $U=2.75$ eV which is very close to the values obtained by a constrained DFT approach,[14] $J=0.79$ and $U=2.7$ eV.

The total energy as a function of the spin moment, as obtained by constraining the staggered spin moments[16] of the stripe ordered AF state, and as a function of U, is displayed in Fig. 1. In agreement with earlier studies[5] the GGA curve ($U=0$) has a clear deep minimum at $m=2.2\mu_B$. This minimum moves slightly to larger moments by increasing U. However, when the spin moment is constrained in the scan for other solutions, we can observe that a second solution starts to develop at a smaller moment. At $U\approx2$ eV this has evolved to a local minimum, which becomes the global minimum for $U\gtrsim2.5$ eV, a value close to the estimated one.[14] At the largest values of the Coulomb parameter also an intermediate minimum is formed. Hence there are several competing metastable states found, among which the low-moment solution is most stable in the case of LaOFeAs and for $U>2$ eV. It is a nontrivial task to find all stable solutions but these are the states we have found after systematic searches. In addition we have verified the low- and large-moment so-

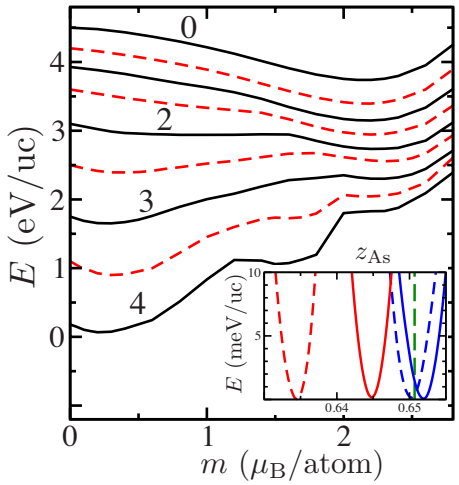

FIG. 1. (Color online) Total energy per magnetic unit cell (4 f.u.) as a function of the staggered spin moment per Fe atom calculated with varying $0 \leq U \leq 4$ eV in steps of 0.5 eV (some values are indicated) with solid curves for integer values. Notice that the energy shifts between the curves are arbitrary and chosen such as to simplify the comparison. In the inset the energy is plotted as a function of z_{As} for $U=0$ (red) with minima at lower z_{As}, nonmagnetic (dashed) and magnetic (full) solutions, and for $U=2.75$ eV (blue), low-spin (dashed) and high-spin (full) solutions. The experimental value (Ref. 6) is indicated by a vertical line.

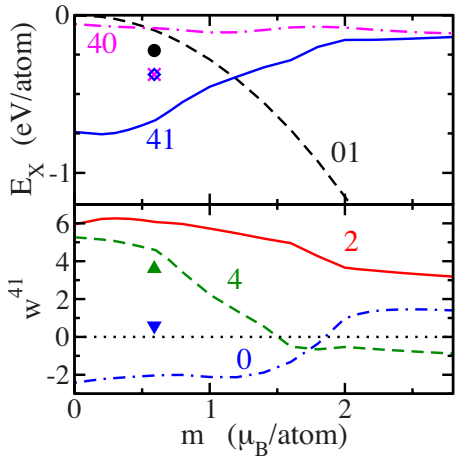

FIG. 2. (Color online) Exchange energy per Fe atom decomposed into multipole $\mathbf{w}^{kp}$ contributions (top, where the number indicates kp) and multipole tensor components w^{41}_{q0} (bottom, with numbers indicating q) as a function of the spin moment per atom for a fixed $U=2.5$ eV. In addition the same quantities are shown with symbols obtained by a corresponding calculation for $CaCuO_2$ with $U=7.0$ eV and calculated $m=0.59\mu_{\mathrm{B}}$.

lutions and their energy difference with an independent code, WIEN2K.[17]

The stabilization energy of the low-moment state is large. Already the high-moment solution of GGA has a significant stabilization energy of 0.17 eV per formula unit (f.u.), for $U=2.5$ eV the low-moment solution is lower than the high-moment solution by 0.04 eV. Both these magnetic solutions have an equilibrium Fe-As bonding distance in close agreement with experiments in stark contrast to the $U=0$ result, as shown in the inset of Fig. 1 for the case of $U=2.75$ eV. Hence, for physical values of U around 2.75 eV the calculations obtain a moment of $0.35\mu_{\mathrm{B}}$ and $z_{\mathrm{As}}=0.650$, both in excellent agreement with experiment.[6] In order to analyze this low-moment solution, that is stabilized at physical values of the Coulomb parameter U, we will adopt the multipole tensor formalism which has been described in detail earlier,[9] but since spin-orbit coupling is of less interest in the present study we will use the uncoupled double tensors. These multipole double tensors can be obtained from the density matrix through[9,18]

$$w^{kp}_{qt} \equiv w_\alpha = \mathrm{Tr}\,\Gamma_\alpha \rho, \tag{1}$$

where the matrix elements of the corresponding expansion matrices Γ_α are given by[9,19]

$$\Gamma^{kp}_{qt;ab} \equiv \Gamma_{\alpha;ab} = N^{-1}_{kp}(-)^{m_a-\ell+s_a-s} \times \mathcal{T}\begin{pmatrix} \ell & k & \ell \\ -m_a & q & m_b \end{pmatrix}\mathcal{T}\begin{pmatrix} s & p & s \\ -s_a & t & s_b \end{pmatrix}, \tag{2}$$

where $\alpha=\{kp;qt\}$ is a composite index for the double tensor indices k and p and the corresponding components q and t, the $(\cdots)$ symbol is the Wigner-3j symbol, and $N_{kp}=n_{\ell k}n_{sp}$, where n is the usual normalization factor.[9,18] The operator $\mathcal{T}$ transforms the spherical tensor, which was used in earlier studies,[19] to a tesseral form.[20] In this study we prefer to work with tesseral tensor moments $\mathbf{w}^{kp}$ since they ensure that the matrices Γ_α are all Hermitian and hence simpler to interpret. The interpretation of these multipole tensors are that for even k they correspond to the multipoles of the charge ($p=0$) or spin magnetization ($p=1$) while for odd k they are multipoles of the corresponding currents. The screened exchange energy takes a very simple and appealing form when expressed in terms of these tensor moments,[9,19]

$$E_{\mathrm{X}} = -\frac{1}{4}\sum_\alpha A_k w^2_\alpha. \tag{3}$$

First, one notes the resemblance with the Stoner exchange, $-Im^2/4$, and indeed one can identify $I=A_0$ since $m=w^{01}_{00}$. Second, all other multipole moments contribute to the screened exchange energy in the exact same way; with an energy parameter times the multipole moment squared. It is to be noted that although the screened exchange is commonly referred to as exchange, it does include important correlation effects.

The exchange contribution to the total energy curve for $U=2.5$ eV of Fig. 1 is decomposed in the contribution from the multipoles $\mathbf{w}^{kp}$, according to Eq. (3) and as displayed in Fig. 2. Besides the spin-polarization energy, which is of course quadratic with the moment, there is a large exchange contribution from the magnetic multipole $\mathbf{w}^{41}$. Since this multipole has the largest magnitude for small moments where it dominates, it is the one that stabilizes the small and intermediate moment solutions for large enough U in Fig. 1. The most significant multipole tensor components w_α as a function of the constrained moment are also displayed in Fig. 2. There exist three independent components of $\mathbf{w}^{41}$: $q=0$, 2,

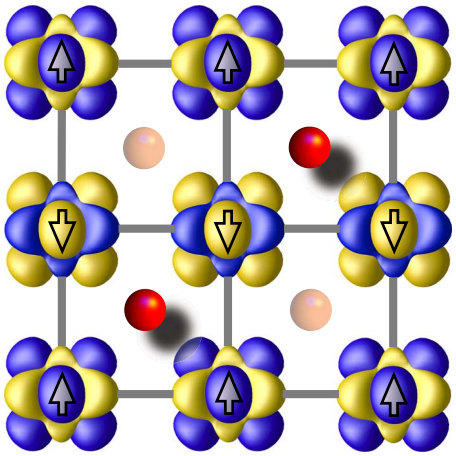

FIG. 3. (Color online) Isosurface plots of the magnetization density around the Fe sites for the striped AF order and $U=2.75$ eV are displayed with positive value indicated with dark/blue and negative with light/yellow. The arrows show the directions of the small integrated atomic dipole moments. The As atoms situated below and above the Fe plane are displayed with spheres.

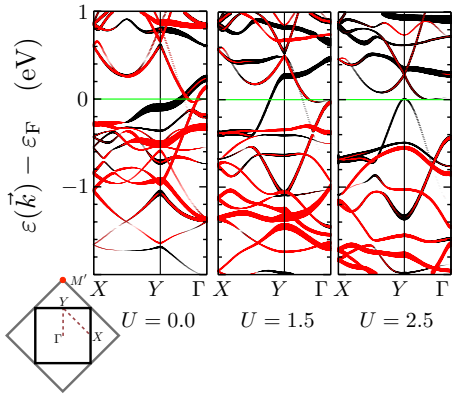

FIG. 4. (Color online) The band structure $\varepsilon(\vec{k})$ along the path X-Y-Γ in the Brillouin zone of the striped AF order (shown in the inset together with the larger nonmagnetic BZ with the corresponding wave vector of the magnetic order M′) for varying Coulomb parameter U and fixed local Fe moment of $0.4\mu_B$. The zero of energy is at the Fermi energy ε_F. The width of the bands are proportional to the expectation value of Γ_{20}^{41} for the band states with the dark/black (light/red) color specifying a negative (positive) value.

and 4. They are the symmetry allowed hexadecapoles (rank 4) of the spin magnetization density which are rotationally invariant, twofold invariant, and fourfold invariant, respectively, around a tetragonal axis through a Fe site. While $q=0$ and 4 are both allowed also for a local tetragonal symmetry, the $q=2$ is permissible due to lower symmetry at the individual Fe sites caused by the striped AF order. These large multipoles result in a very anisotropic magnetization density as seen in Fig. 3 for the case of $U=2.75$ eV, where the magnetization density has both large positive and negative values but integrates to a small value of $0.35\mu_B$. Such multipoles could be detected by, e.g., resonant x-ray scattering experiments.[21]

This low-moment solution is stabilized through an intricate competition between gain in screened exchange energy and loss in kinetic energy. The gain in exchange energy by the Coulomb interaction of Eq. (3) is manifested in the orbital-dependent exchange potential matrix which enters the LDA+U Hamiltonian,

$$V_X = \frac{\partial E_X}{\partial \rho^T} = \sum_\alpha \frac{\partial E_X}{\partial w_\alpha}\frac{\partial w_\alpha}{\partial \rho^T} = -\frac{1}{2}\sum_\alpha A_k w_\alpha \Gamma_\alpha. \tag{4}$$

Again, since $\Gamma_{00}^{01}=1\otimes\sigma_z$, it is possible to identify the Stoner exchange splitting $\Delta_S=Im=A_0 w_{00}^{01}$, that can be generalized to the higher multipole splitting $\Delta_\alpha=A_k w_\alpha$. The corresponding Γ_α matrix describes which kind of states will split due the multipole α and generally involves the orbital degrees of freedom. The Γ matrix for the most significant component of the magnetic multipole, in the orbital basis of xz, yz, xy, x^2-y^2, and z^2, is given by

$$\Gamma_{20}^{41} = \begin{pmatrix} 2\sqrt{5} & 0 & 0 & 0 & 0 \\ 0 & -2\sqrt{5} & 0 & 0 & 0 \\ 0 & 0 & 0 & 0 & 0 \\ 0 & 0 & 0 & 0 & \sqrt{15} \\ 0 & 0 & 0 & \sqrt{15} & 0 \end{pmatrix} \otimes \sigma_z, \tag{5}$$

where σ_z is the Pauli spin matrix. Hence, the existence of w_{20}^{41} moments manifests an ordering of spin orbitals, by, e.g., a spin-dependent splitting of the xz and yz Fe d orbitals. For anisotropic band structures, as in this case, this polarization acts with higher precision on the relevant bands around the Fermi energy than the uniform spin polarization. Spin-orbital orderings of a slightly different form has recently been discussed in LaOFeAs.[22]

In Fig. 4 the band structures are displayed for three different values of U with the local staggered magnetic moment constrained to a value representative to low-moment solution, $0.4\mu_B$. The $\vec{k}$ path is in the basal plane of the BZ as shown in Fig. 4. The two points X and Y become equivalent in the case of time reversal (TR) symmetry. First, we will take a look at the GGA ($U=0$) solutions. One can see the nesting features of the bands at the Fermi energy along the YΓ line. These bands originate from the hole Fermi surface around the Γ point and the electron Fermi surfaces downfolded from the M′ point of the larger TR symmetric BZ.[23] Surprisingly, these bands seem to be inert to the nesting effect since the bands cross also in the AF structure with no hybridization gap opening up. This is due to the different orbital character of these nested bands.

Now, we will focus on the stabilization of the low-moment solution due to the formation of multipoles. For finite U one can see that the bands become polarized through the action of the orbital-dependent potential of Eq. (4), as illustrated by the "fatness" and color of the plotted bands in Fig. 4. The width is proportional to the magnitude of the

expectation value of the matrix Γ_{20}^{41} with light and dark colors indicating positive and negative values. Here we can see that there are large splittings due to the polarization of the w_{20}^{41} tensor components, which results in strong rearrangements, especially along the YΓ line. This produces a large asymmetry along the XY line. This splitting together with the one of the w_{40}^{41} tensor components leads to an effective opening of a pseudogap at the Fermi energy and a stabilization of this low-moment solution. For larger $U>4$ eV, this effect is so strong that a true gap opens up and the solution becomes insulating. Again, as is clear from the intermediate $U=1.5$ eV plot, the Fermi-surface nesting has no direct role in the stabilization of this low-moment solution, which is in agreement with a recent angular-resolved photoemission spectroscopy experiment.[24]

Finally, we want to underline the fact that the multipole needed to stabilize the low-moment solution, instead of the large-moment solution as predicted by GGA, also plays a crucial role in the formation of an insulating AF solution in the cuprates, as, e.g., $CaCuO_2$. The multipoles and their energies for $CaCuO_2$ calculated with $U=7.0$ eV are shown in Fig. 2. In this case the existence of the multipole is easier to understand as it is essentially a pure x^2-y^2 orbital that polarizes, giving arise to a nonspherical charge and magnetization density. However, the magnitude of the multipoles are of the same order as in LaOFeAs, and in fact, without these multipoles, the nonmagnetic solution is more stable. This finding is in accordance with the fact that more exchange energy goes into the formation of the multipole than that of the spin moment. Hence, in both types of compounds it is the neglect of these multipole exchange channels in LDA and GGA that leads to the wrong ground state with either too large (LaOFeAs) or too small moments ($CaCuO_2$). This favorable comparison between the magnetism of the undoped LaOFeAs and an undoped cuprate will be explored in further details in a future study. Then a crucial issue remains wide open; how do these spin- and spin-orbital-ordered AF ground states of the parent compound, with their significant formation energies, vanish already with a small doping, which eventually leads to a high-T_C superconductivity? One can speculate that the multipole order in some form remains beyond the doping where the AF order is destroyed, and then constitutes the hidden order of the so-called pseudogap region, which is well established in the cuprates[25] and has been observed recently for the pnictides.[26]

The support from the Swedish Research Council (VR) is thankfully acknowledged. The computer calculations have been performed at HPC2N and NSC under grant provided by the Swedish National Infrastructure for Computing (SNIC).

[1] Y. Kamihara *et al.*, J. Am. Chem. Soc. **130**, 3296 (2008).
[2] M. R. Norman, Phys. **1**, 21 (2008).
[3] Z. Tesanovic, Phys. **2**, 60 (2009).
[4] V. I. Anisimov, J. Zaanen, and O. K. Andersen, Phys. Rev. B **44**, 943 (1991).
[5] I. I. Mazin, M. D. Johannes, L. Boeri, K. Koepernik, and D. J. Singh, Phys. Rev. B **78**, 085104 (2008).
[6] C. de la Cruz *et al.*, Nature (London) **453**, 899 (2008).
[7] I. Opahle, H. C. Kandpal, Y. Zhang, C. Gros, and R. Valenti, Phys. Rev. B **79**, 024509 (2009).
[8] http://elk.sourceforge.net
[9] F. Bultmark, F. Cricchio, O. Granas, and L. Nordstrom, Phys. Rev. B **80**, 035121 (2009).
[10] M. R. Norman, Phys. Rev. B **52**, 1421 (1995).
[11] J. P. Perdew, K. Burke, and M. Ernzerhof, Phys. Rev. Lett. **77**, 3865 (1996).
[12] K. Haule, J. H. Shim, and G. Kotliar, Phys. Rev. Lett. **100**, 226402 (2008).
[13] V. I. Anisimov *et al.*, J. Phys.: Condens. Matter **21**, 075602 (2009).
[14] M. Aichhorn, L. Pourovskii, V. Vildosola, M. Ferrero, O. Parcollet, T. Miyake, A. Georges, and S. Biermann, Phys. Rev. B **80**, 085101 (2009).
[15] W. Yang *et al.*, Phys. Rev. B **80**, 014508 (2009).
[16] P. H. Dederichs, S. Blugel, R. Zeller, and H. Akai, Phys. Rev. Lett. **53**, 2512 (1984).
[17] K. Schwarz and P. Blaha, Comput. Mater. Sci. **28**, 259 (2003).
[18] G. Laan and B. Tholet, J. Phys.: Condens. Matter **7**, 9947 (1995).
[19] F. Cricchio, F. Bultmark, and L. Nordström, Phys. Rev. B **78**, 100404(R) (2008).
[20] A tesseral tensor x^r is related to the spherical tensor $\tilde{x}^r$ through $x_0^r=\tilde{x}_0^r$ and $x_q^r=[\tilde{x}_{|q|}^r+(-)^q\tau\tilde{x}_{-|q|}^r]/\sqrt{2\tau}$ for $q\neq 0$, where $\tau=\mathrm{sgn}\ q$.
[21] J. Fernandez-Rodríguez, V. Scagnoli, C. Mazzoli, F. Fabrizi, S. W. Lovesey, J. A. Blanco, D. S. Sivia, K. S. Knight, F. de Bergevin, and L. Paolasini, Phys. Rev. B **81**, 085107 (2010).
[22] F. Krüger, S. Kumar, J. Zaanen, and J. van den Brink, Phys. Rev. B **79**, 054504 (2009).
[23] D. J. Singh and M.-H. Du, Phys. Rev. Lett. **100**, 237003 (2008).
[24] G. Liu *et al.*, Phys. Rev. B **80**, 134519 (2009).
[25] T. Timusk and B. Statt, Rep. Prog. Phys. **62**, 61 (1999).
[26] T. Kato, Y. Mizuguchi, H. Nakamura, T. Machida, H. Sakata, and Y. Takano, Phys. Rev. B **80**, 180507(R) (2009).